

## **Supporting Information**

### **Edge vs. Basal Plane of $\text{Ti}_3\text{C}_2\text{T}_x$ MXene: Enhanced Inherent Electrochemistry, Electron Transfer, and Catalytic Activity at the Edge**

Shubham Upadhye,<sup>a</sup> Gopal K. Pradhan,<sup>b</sup> Pranati Nayak <sup>a\*</sup>

<sup>a</sup> Department of Engineering and Materials Physics, Institute of Chemical Technology-Indian Oil Odisha Campus, Bhubaneswar 751013, India

<sup>b</sup> Department of Physics, School of Applied Science, KIIT Deemed to be University, Bhubaneswar, India

### **Experimental Section**

#### **Materials & Chemicals**

For electrochemical measurements, a saturated calomel reference and Pt wire counter electrodes, procured from CH Instruments, USA, were used. Membrane filter papers of pore size 0.22  $\mu\text{m}$  were bought from Merck. All the chemicals were of analytical grade and were used as received without further purification. Ascorbic acid was procured from Merck, Germany. Potassium hydroxide (KOH), potassium chloride (KCl), hydrochloric acid (HCl), Hydrofluoric acid(HF), sulphuric acid ( $\text{H}_2\text{SO}_4$ ), lithium chloride (LiCl), sodium hydroxide (NaOH), dopamine hydrochloride- $[(\text{HO})_2\text{C}_6\text{H}_3\text{CH}_2\text{CH}_2\text{NH}_2\cdot\text{HCl}]$ , sodium phosphate dibasic heptahydrate( $\text{Na}_2\text{HPO}_4\cdot 7\text{H}_2\text{O}$ ), sodium phosphate monobasic monohydrate( $\text{NaH}_2\text{PO}_4\cdot \text{H}_2\text{O}$ ), hexaammineruthenium (III) chloride( $[\text{Ru}(\text{NH}_3)_6]\text{Cl}_3$ ) & potassium hexacyanoferrate ( $\text{K}_4\text{Fe}(\text{CN})_6\cdot 3\text{H}_2\text{O}$ ) were all procured from Sigma-Aldrich, Germany. Titanium aluminum carbide ( $\text{Ti}_3\text{AlC}_2$ , 98%, 200 mesh) powders were purchased from Beijing HWRK Chem Co., Ltd. All the solutions used for the electrochemical measurements were prepared using ultrapure water (18.2 M $\Omega$  cm, Merck Millipore, MA) without any further purification. SYLGARD 184 silicone elastomer was mixed in the ratio of 10:1 (base & curing agent, respectively) & was kept in a vacuum to remove any air bubbles present in it before it was used for defining the surface area of the working electrode.

#### **Material synthesis & electrode fabrication**

$\text{Ti}_3\text{C}_2\text{T}_x$  was prepared using a typical etching method with HF, following the guidelines for MXene synthesis.<sup>33</sup> Specifically, 1 g of  $\text{Ti}_3\text{AlC}_2$  powder was added to 30 ml of (HF + HCl) and stirred for 24 h at 40 °C. The dispersants were then centrifuged at 3500 rpm for 30 min and washed repeatedly with deionized water until a pH of approximately 6 was reached. Then, the standard procedures were followed to delaminate the bulk MXenes. The collected supernatant was stored for characterization and electrode fabrication. To prepare the MXene free-standing film, a calculated amount of supernatant was allowed to filter using a vacuum filtration setup followed by drying under vacuum.

To fabricate basal plane and edge-oriented  $Ti_3C_2Tx$  MXene electrodes, the  $Ti_3C_2Tx$  MXene free-standing film was cut into a 2 mm x 5mm size. Further, the film was attached to a conducting wire using conducting silver paint. To prepare an edge-oriented electrode, the passivated film was cut across the edge, resulting in exposed edge plane sites. In contrast, to prepare basal plane electrodes, a selective area over the film surface was left uncoated, leaving the rest of the area passivated conformally by elastomers. The whole fabrication procedure is represented in **Figure 1** of the main manuscript. The exposed surface area of edge plane electrodes was obtained from FESEM, while the basal plane area was determined by using IMAGE ImageJ software.

### **Material/Electrode Characterization**

The surface morphology of the prepared MXene film electrodes was characterized using a field emission scanning electron microscope (FESEM, Zeiss Gemini 450) operating at 20 kV. Powder X-ray diffraction (P-XRD, D8 ADVANCE powder X-ray diffractometer with  $Cu K\alpha$  radiation ( $\lambda = 0.154$  nm, Bruker) was used to evaluate the crystallinity of the samples. Raman spectra analysis was executed on a confocal Raman spectrometer (Renishaw) with a CCD detector, using an argon ion laser (excitation wavelength 633 nm) and a 100x objective lens. The spot size of the laser was fixed at 5  $\mu m$  diameter. The calibration was performed with silicon as a reference at  $520\text{ cm}^{-1}$ . The deconvolution of Raman spectra was done using Origin software.

### **Electrochemical studies**

All the electrochemical measurements were carried out using a Metrohm Autolab electrochemical workstation (PGSTAT302N, Netherlands) with NOVA software version 2.1.7. Electrochemical measurements were done in a 20 ml voltammetric cell equipped with a three-electrode configuration with a commercial Pt wire as auxiliary electrode and a saturated calomel as the reference electrode. The fabricated MXene film electrodes (both edge plane and basal plane) were used as the working electrode.

### **Inherent electrochemistry and charge Transfer studies on edge and basal plane $Ti_3C_2Tx$ MXene electrodes**

The fundamental electrochemistry and charge transfer mechanism studies were carried out by performing cyclic voltammetry (CV) experiments in different background electrolyte conditions. All the CVs were performed at 100 mV/s scan rates. The as-prepared MXene edge and basal plane electrodes were used directly without any surface treatment. In a complete cycle, the CV was allowed to start from 0V, where no redox processes are expected to happen, towards higher +ve potential, followed by a reverse sweep to higher -ve end and then back to 0V. Three repeated scans were performed for each CV measurement. The Heterogeneous electron transfer (HET) studies were performed using CVs at varying scan rates (10-500 mV/s) in the presence of both inner (5 mM  $K_4[Fe(CN)_6]$ ) and outer (5 mM  $[Ru(NH_3)_6]Cl_3$ ) sphere redox probes in 0.1 M KCl as the supporting electrolyte.

The  $k^0$  values were calculated using the method developed by Nicholson (41 which relates the  $\Delta E_p$  value to a dimensionless parameter, “ $\Psi$ ,” and the HET rate constant,  $k^0$ . To compute the  $k^0$  values, the diffusion coefficient values were taken from literature:  $D = 6.7 \times 10^{-6} \text{ cm}^2/\text{s}$  for  $[\text{Fe}(\text{CN})_6]^{4-}$  and  $D = 8.43 \times 10^{-6} \text{ cm}^2/\text{s}$  for  $[\text{Ru}(\text{NH}_3)_6]^{3+}$ , respectively.

#### **Catalytic activity and hydrogen evolution reaction (HER) studies on the edge and basal plane $\text{Ti}_3\text{C}_2\text{T}_x$ MXene electrodes.**

The catalytic activity of the edge plane  $\text{Ti}_3\text{C}_2\text{T}_x$  MXene electrodes over the basal planes towards analytes such as dopamine and ascorbic acid was evaluated using differential pulse voltammetry (DPV). The hydrogen evolution reaction (HER) efficiency of the edge plane vs. the basal plane was evaluated using linear sweep voltammetry (LSV) at a scan rate of 5 mV/s in 0.5 mM  $\text{H}_2\text{SO}_4$  as electrolyte. All experiments were conducted in a controlled thermostatic environment ( $25 \pm 1^\circ\text{C}$ ). The deoxygenation of all the electrolyte solutions was performed before the commencement of the electrochemical measurements.

Figure S1

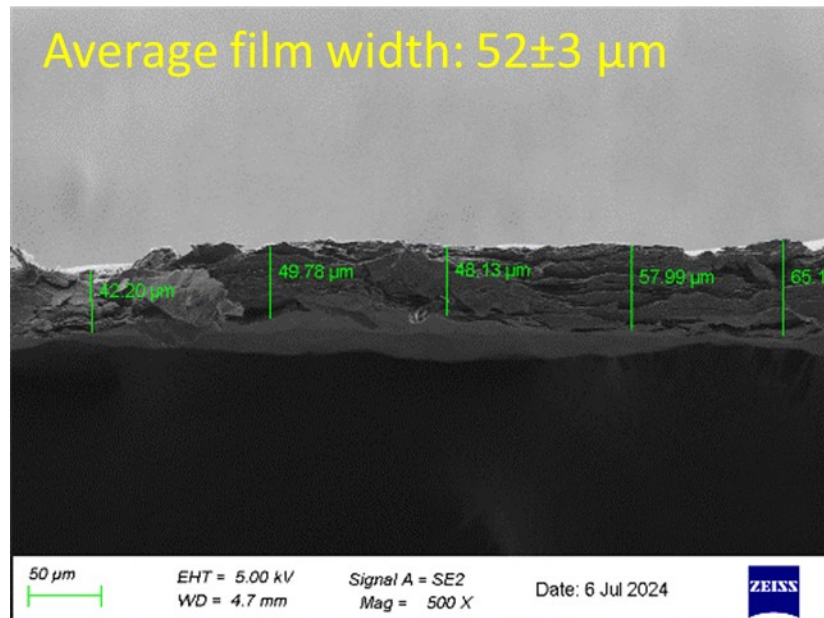


Figure S1. FESEM image of the edge of  $\text{Ti}_3\text{C}_2\text{T}_x$  MXene free standing film

Figure S2

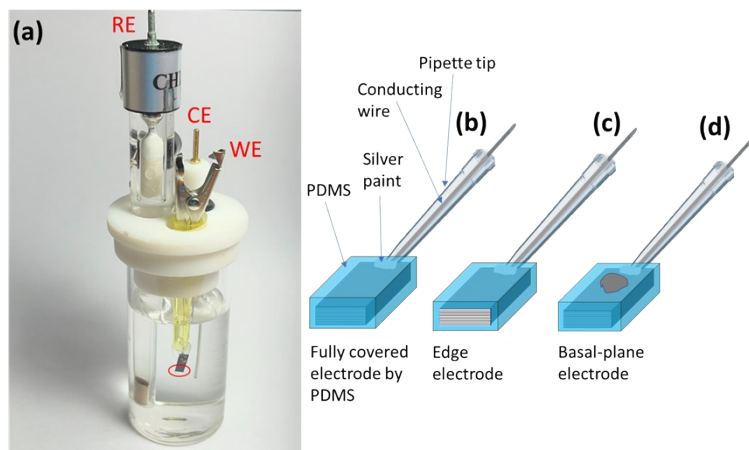


Figure S2(a) three-electrode set-up in an electrochemical cell, (b-d) complete fabrication of edge and basal plane electrodes.

Figure S3

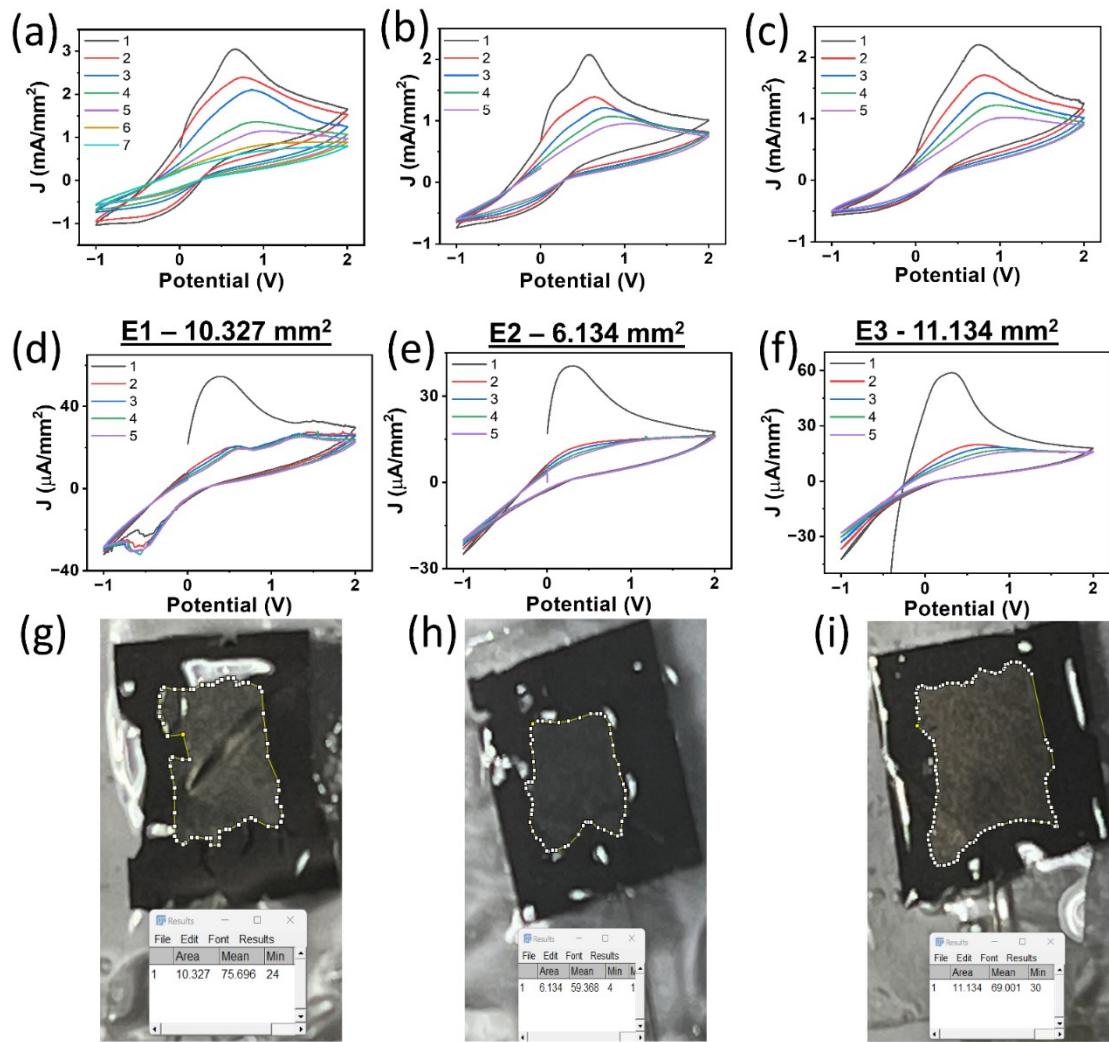


Figure S3: Cyclic voltammograms for the three different edge plane (a, b, c) & basal plane (d, e, f)  $\text{Ti}_3\text{C}_2\text{T}_x$  film electrodes in 0.1M KOH electrolyte. Digital photographs of the basal plane electrodes with defined working area calculation using IMAGE J software (g, h, i). Conditions: Scan rate, 100 mV/s; all measurements are performed relative to the saturated calomel reference electrode and thermostatic conditions at temperature  $25^\circ\text{C} \pm 1^\circ\text{C}$ .

Figure S4

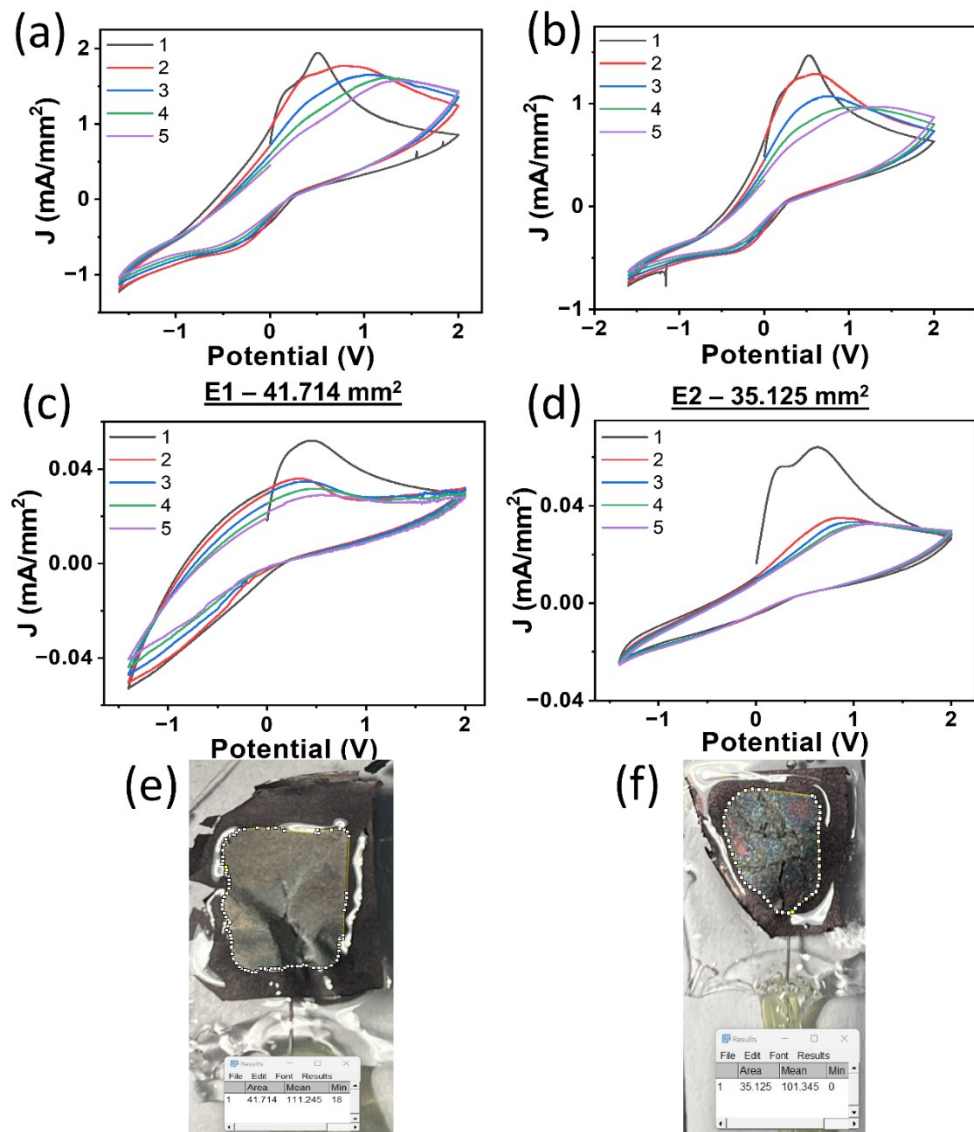


Figure S4: Cyclic voltammograms for the two different edge plane (a, b) & basal plane (c, d)  $\text{Ti}_3\text{C}_2\text{Tx}$  film electrodes in 0.1M NaOH electrolyte. Digital photographs of the basal plane electrodes with defined working area calculation using IMAGE J software (e, f). Conditions: Scan rate, 100 mV/s; all measurements are performed relative to the saturated calomel reference electrode and thermostatic conditions at temperature  $25^\circ\text{C} \pm 1^\circ\text{C}$ .

Figure S5

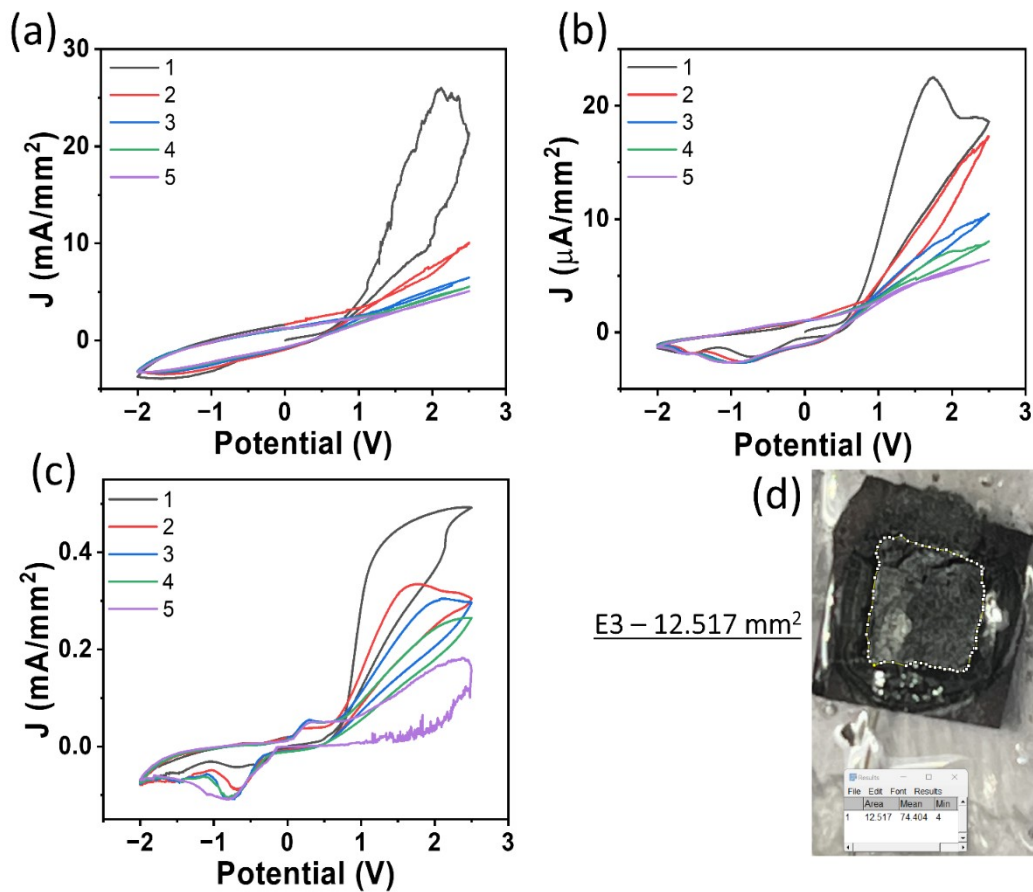


Figure S5. Cyclic voltammograms for the two different edge plane (a, b) & basal plane (c)  $\text{Ti}_3\text{C}_2\text{T}_x$  film electrodes in 0.1M KCl electrolyte. Digital photographs of the basal plane electrodes with defined working area calculation using IMAGE J software (d). Conditions: Scan rate, 100 mV/s; all measurements are performed relative to the saturated calomel reference electrode and thermostatic conditions at temperature  $25^\circ\text{C} \pm 1^\circ\text{C}$

Figure S6

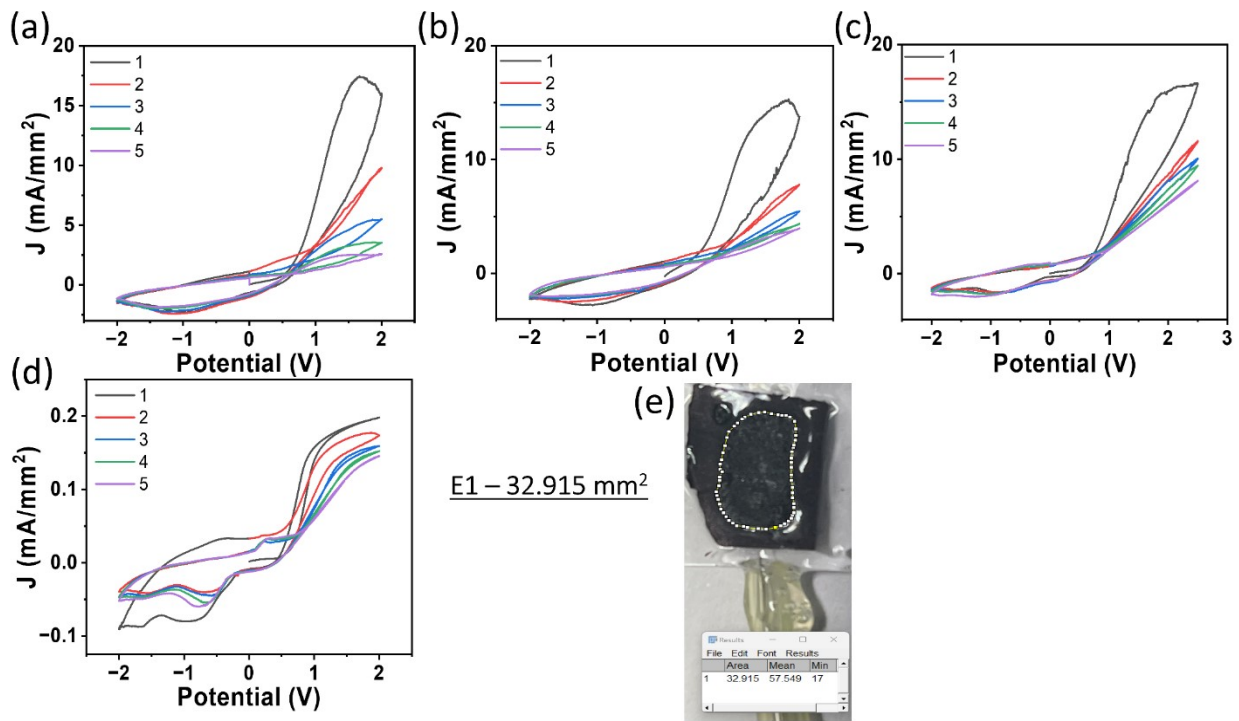


Figure S6: Cyclic voltammograms for the three different edge plane (a, b, c) & basal plane (d)  $\text{Ti}_3\text{C}_2\text{T}_x$  film electrodes in 0.1M LiCl electrolyte. Digital photographs of the basal plane electrodes with defined working area calculation using IMAGE J software (e). Conditions: Scan rate, 100 mV/s; all measurements are performed relative to the saturated calomel reference electrode and thermostatic conditions at temperature  $25^\circ\text{C} \pm 1^\circ\text{C}$ .

Figure S7

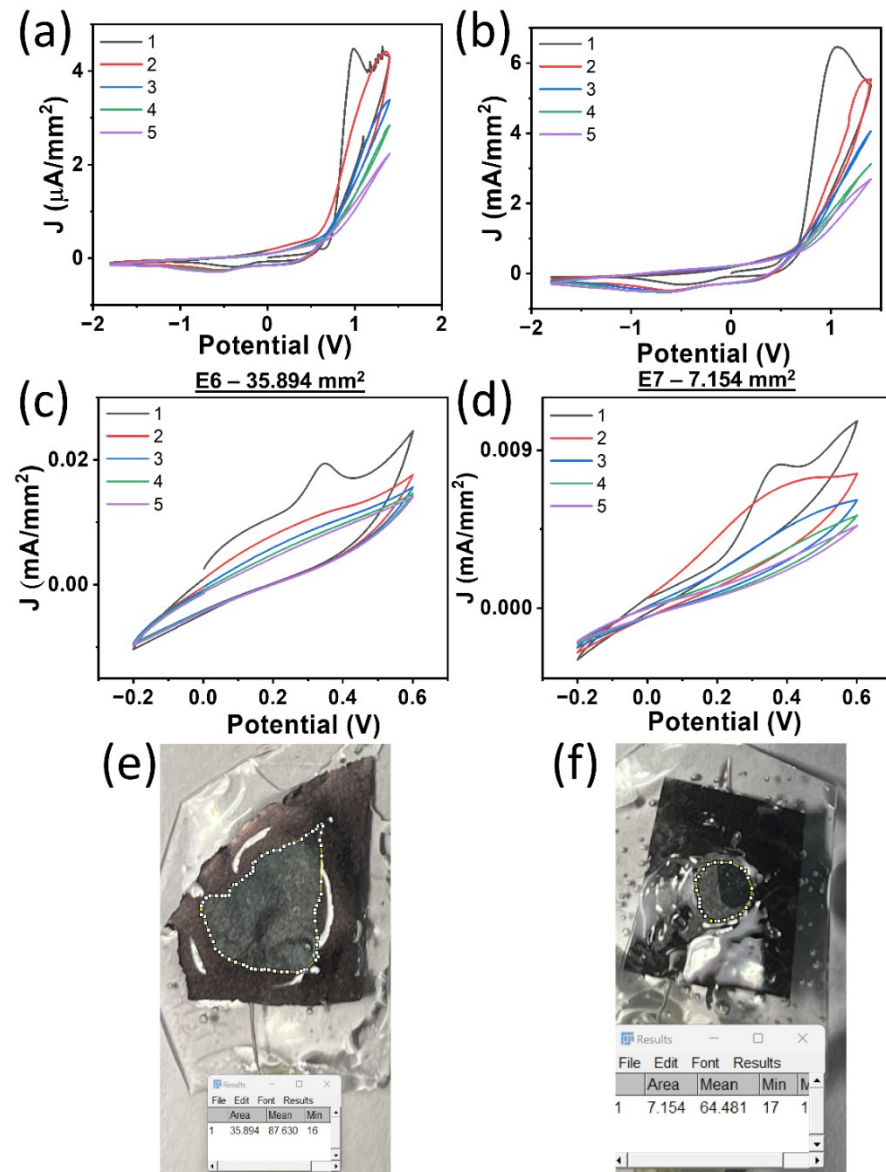


Figure S7. Cyclic voltammograms for the two different edge plane (a, b) & basal plane (c, d)  $\text{Ti}_3\text{C}_2\text{T}_x$  film electrodes in 0.1M PBS electrolyte. Digital photographs of the basal plane electrodes with defined working area calculation using IMAGE J software (e, f). Conditions: Scan rate, 100 mV/s; all measurements are performed relative to the saturated calomel reference electrode and thermostatic conditions at temperature  $25^\circ\text{C} \pm 1^\circ\text{C}$ .

Figure S8

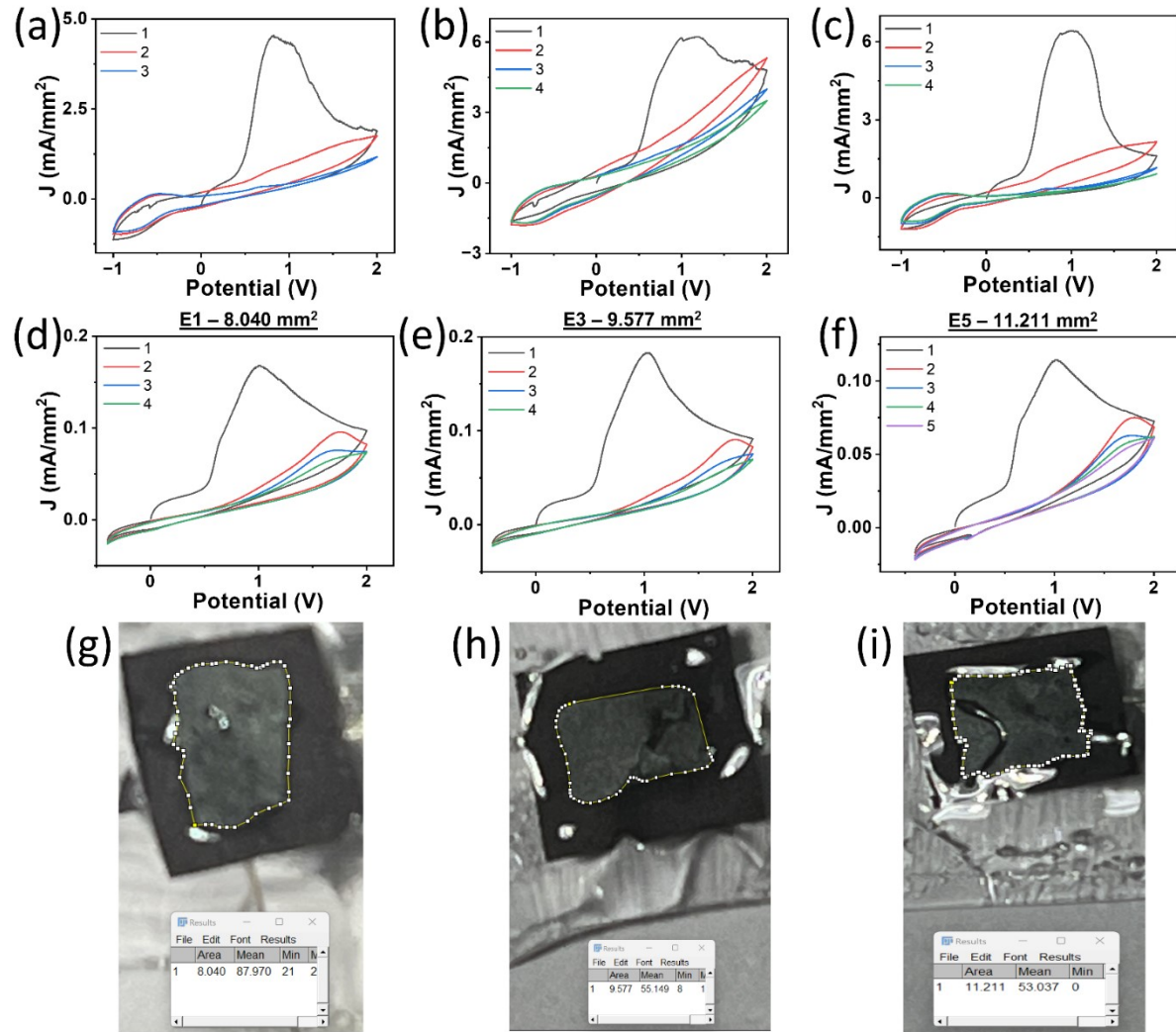


Figure S8. Cyclic voltammograms for the three different edge plane (a, b, c) & basal plane (d, e, f)  $\text{Ti}_3\text{C}_2\text{T}_x$  film electrodes in 0.1M  $\text{H}_2\text{SO}_4$  electrolyte. Digital photographs of the basal plane electrodes with defined working area calculation using IMAGE J software (g, h, i). Conditions: Scan rate, 100 mV/s; all measurements are performed relative to the saturated calomel reference electrode and thermostatic conditions at temperature  $25^\circ\text{C} \pm 1^\circ\text{C}$ .

Figure S9

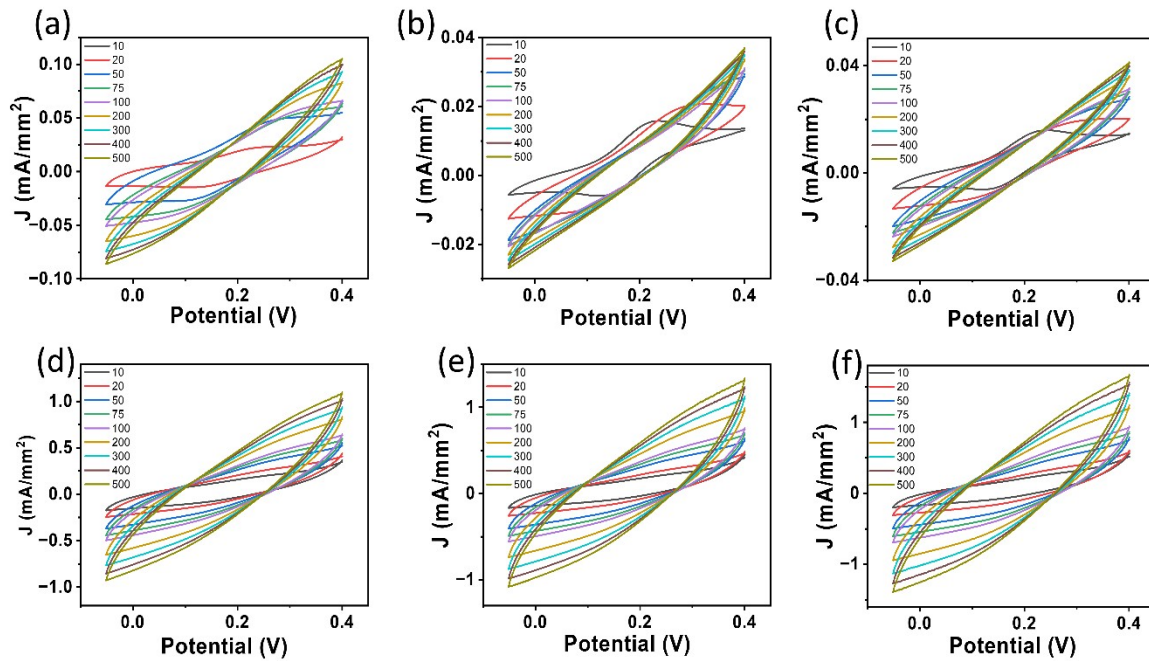


Figure S9. Cyclic voltammograms for the three different edge plane (a, b, c) & basal plane (d, e, f)  $\text{Ti}_3\text{C}_2\text{T}_x$  film electrodes in 0.1M KCl electrolyte containing 20 mM  $\text{K}_4\text{Fe}(\text{CN})_6 \cdot 3\text{H}_2\text{O}$  redox probe. Conditions: Scan rate, 100 mV/s; all measurements are performed relative to the saturated calomel reference electrode and thermostatic conditions at temperature  $25^\circ\text{C} \pm 1^\circ\text{C}$

Figure S10

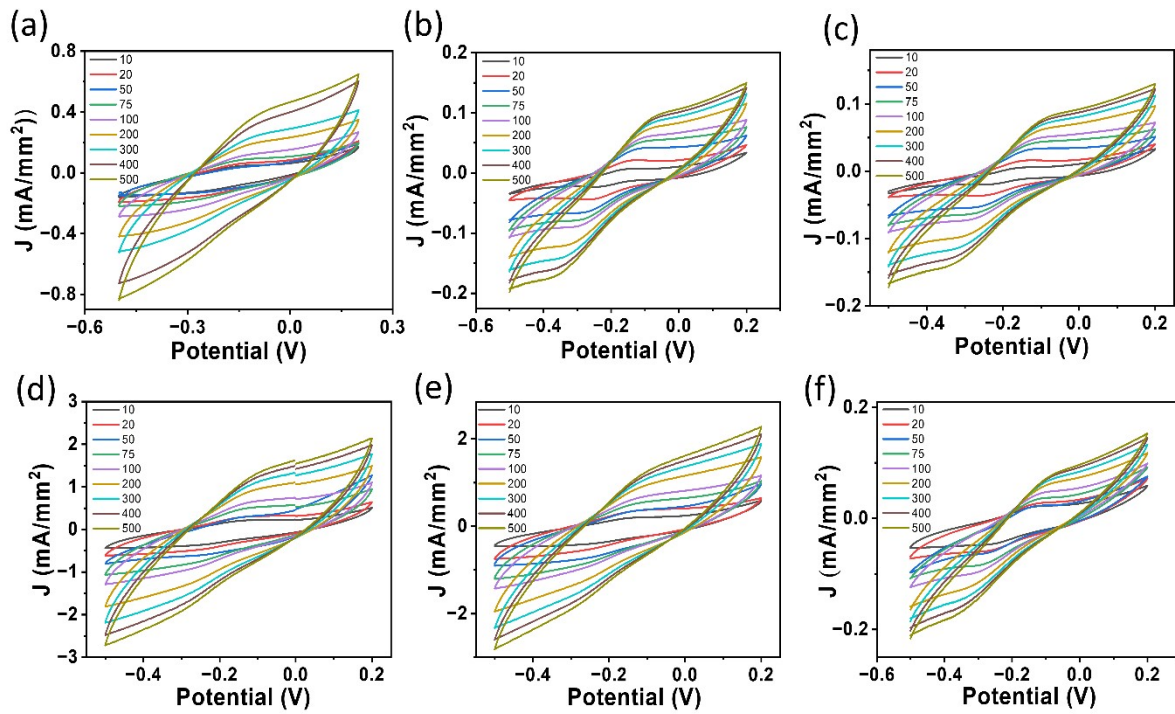


Figure S10. Cyclic voltammograms for the three different edge plane (a, b, c) & basal plane (d, e, f)  $\text{Ti}_3\text{C}_2\text{T}_x$  film electrodes in 0.1M KCl electrolyte containing 20 mM  $[\text{Ru}(\text{NH}_3)_6]\text{Cl}_3$  redox probes. Conditions: Scan rate, 100 mV/s; all measurements are performed relative to the saturated calomel reference electrode and thermostatic conditions at temperature  $25^\circ\text{C} \pm 1^\circ\text{C}$ .

Figure S11

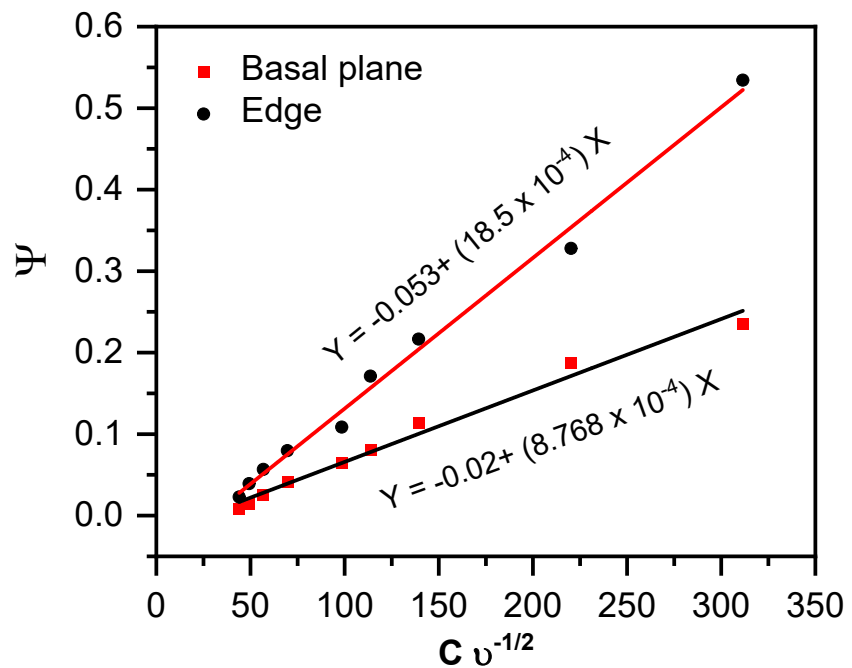


Figure S11. Plot of Nicholson's kinetic parameter  $\Psi$  versus  $C$  multiplied by the reciprocal of the square root of the potential scan rate ( $Cv^{-1/2}$ ) for both edge and basal plane MXene electrodes. Linear fitting is used to calculate the standard HET rate ( $k^0$ ).

Figure S12

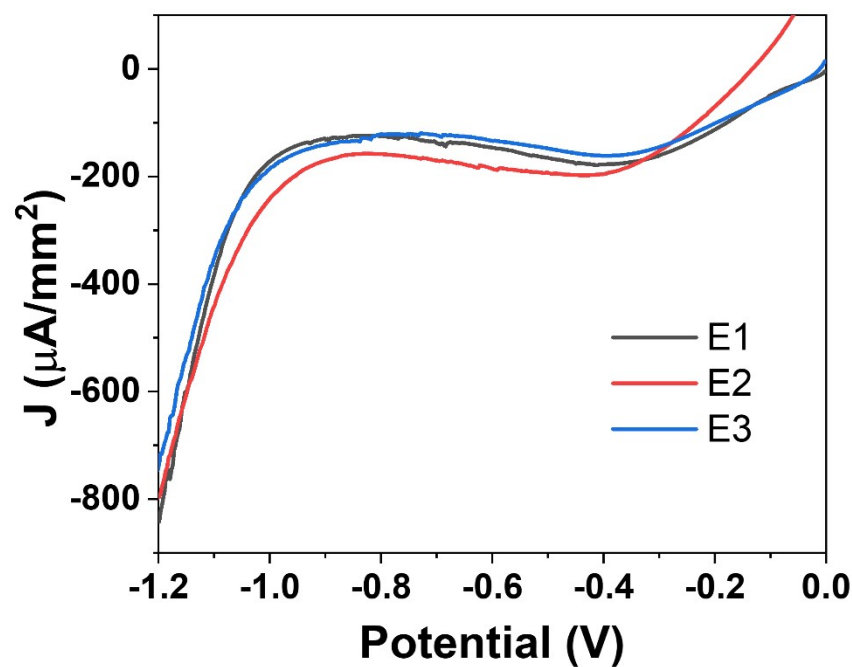


Figure S12. Linear Sweep Voltammetry (LSV) representing the HER performance study of the three different edge plane electrodes in 0.1M H<sub>2</sub>SO<sub>4</sub> electrolyte. LSV measurements were performed at 5 mV/s under thermostatic conditions (temperature: 25 °C ± 1 °C).